



OPTIMIZATION OF COMPOSITE SHELLS

Alexandre Kaelble Calixto

Universidade Federal de Santa Catarina, UFSC

Dep. Engenharia Mecânica, CP 476, Florianópolis, SC, 88010-970

Marcelo Krajnc Alves

Universidade Federal de Santa Catarina, UFSC

Dep. Engenharia Mecânica, CP 476, Florianópolis, SC, 88010-970

Abstract. *In this work we propose an algorithm for the analysis and optimization of composite shell structures. The laminate composite material is formed by the superposition of several orthotropic layers, each constituted by unidirectional fibers in an epoxy matrix. The laminate is modeled through the theory of the equivalent layer which is obtained by the classical rule of mixtures. Here we consider shells of double curvature which are modeled by the higher order theory presented by (Kant, 1982). The objective, here, is to minimize the weight of the structure obtaining the optimum thickness and fibers directions for each layer that forms the laminate. The design variables are considered to have side constraints and the effective stresses, in the baricenter of each element, to be bounded by some admissible stress limit.*

Key words: *Composite Material, Shell, Optimization*

1. INTRODUCTION

The use of composite materials had a considerable increment in the last few years becoming more and more a feasible alternative to the standard materials. This is due mainly to the high strength and low weight and the possibility to control the composite layers in order to obtain customized materials with the desired properties. Parameters such as orientation of fibers, sequence of piling up of the laminates, fiber and matrix type may be determined in an optimal way. The mechanical characteristics and properties turn them extremely attractive for a great variety of industrial applications, in the naval, aeronautics, aerospace and defense industries. The classical theories of thin shells shows enormous discrepancy when used in the analysis of plates and laminated shells of composite materials, showing that these theories are inadequate for modeling these problems. However, (Pandya and Kant, 1988) have shown that high order theories improve considerably the results when compared with experimental data.

2. SHELL THEORY

In this work we make use of the classical higher order theory proposed by (Kant, 1982) which considers a displacement field, at a point q , to be given by the following components: (Batoz and Dhatt, 1992)

$$\begin{aligned}
u_q(\xi, \eta, \varsigma) &= u(\xi, \eta) + \varsigma \theta_2(\xi, \eta) + \varsigma^3 \theta_2^*(\xi, \eta), \\
v_q(\xi, \eta, \varsigma) &= v(\xi, \eta) + \varsigma \theta_1(\xi, \eta) + \varsigma^3 \theta_1^*(\xi, \eta), \\
w_q(\xi, \eta, \varsigma) &= w(\xi, \eta) + \varsigma^2 w^*(\xi, \eta),
\end{aligned} \tag{1}$$

where u and v are the plane membrane displacements, w is the traverse displacement of a point on the reference surface, θ_x and θ_y are the rotations of the normal to the reference plane around the axes y and x , respectively. The parameters w^* , θ_x^* and θ_y^* are associated with w , θ_x and θ_y and related to the higher order theory.

2.1 Principle of virtual work

Let Ω be the domain of a generic body. Then, the principle of virtual work is given, by: $W_{(i)} + W_{(e)} = 0$, $\forall \hat{u} \in Var_u$. The work of the external forces is given by:

$$W_{(e)} = \int_{\Gamma_f} (\hat{u} \cdot \bar{f} + \hat{\theta} \cdot \bar{M} + \hat{u}^* \cdot \bar{f}^* + \hat{\theta}^* \cdot \bar{M}^*) dS \tag{2}$$

with

$$(\bar{f}, \bar{M}, \bar{f}^*, \bar{M}^*) = \sum_{k=1}^n \int_{h_i}^{h_{i+1}} (1, \varsigma, \varsigma^2, \varsigma^3) \bar{f} dS,$$

where \bar{f} is the prescribed traction of the boundary Γ_f . The work of the internal forces is

$$W_{(i)} = \int_A \{ N \cdot \hat{\epsilon} + M \cdot \hat{\chi} + N^* \cdot \hat{\epsilon}^* + M^* \cdot \hat{\chi}^* + Q \cdot \hat{\gamma} + Q^* \cdot \hat{\gamma}^* + Q^{**} \cdot \hat{\gamma}^{**} + N_n \cdot \hat{\epsilon}_n \} dA, \tag{3}$$

where A denotes the mid-surface, $(\hat{\epsilon}, \hat{\chi}, \hat{\epsilon}^*, \hat{\chi}^*, \hat{\gamma}, \hat{\gamma}^*, \hat{\gamma}^{**}, \hat{\epsilon}_n)$ are the classical generalized "strains" and $(N, M, N^*, M^*, Q, Q^*, Q^{**}, N_n)$ "stresses". The generalized "strains" may be expressed as:

$$\begin{aligned}
\hat{\epsilon} &= \begin{bmatrix} \hat{\epsilon}_{xx} & \hat{\epsilon}_{xy} \\ \hat{\epsilon}_{yx} & \hat{\epsilon}_{yy} \end{bmatrix}, \quad \hat{\epsilon}^* = \begin{bmatrix} \hat{\epsilon}_{xx}^* & \hat{\epsilon}_{xy}^* \\ \hat{\epsilon}_{yx}^* & \hat{\epsilon}_{yy}^* \end{bmatrix}, \\
\hat{\chi} &= \begin{bmatrix} \hat{\chi}_{xx} & \hat{\chi}_{xy} \\ \hat{\chi}_{yx} & \hat{\chi}_{yy} \end{bmatrix}, \quad \hat{\chi}^* = \begin{bmatrix} \hat{\chi}_{xx}^* & \hat{\chi}_{xy}^* \\ \hat{\chi}_{yx}^* & \hat{\chi}_{yy}^* \end{bmatrix}, \quad \hat{\gamma} = \begin{bmatrix} \hat{\gamma}_{xz} \\ \hat{\gamma}_{yz} \end{bmatrix}, \\
\hat{\gamma}^* &= \begin{bmatrix} \hat{\gamma}_{xz}^* \\ \hat{\gamma}_{yz}^* \end{bmatrix} \quad \text{and} \quad \hat{\gamma}^{**} = \begin{bmatrix} \hat{\gamma}_{xz}^{**} \\ \hat{\gamma}_{yz}^{**} \end{bmatrix}.
\end{aligned} \tag{4}$$

The generalized "stresses" may be expressed as:

$$N = \sum_{k=1}^n \int_{h_i}^{h_{i+1}} \Lambda \sigma^S d\varsigma, \quad N^* = \sum_{k=1}^n \int_{h_i}^{h_{i+1}} \Lambda \sigma^S \varsigma^2 d\varsigma,$$

$$\begin{aligned}
\mathbf{M} &= \sum_{k=1}^n \int_{h_i}^{h_{i+1}} \Lambda \sigma^S \zeta d\zeta, & \mathbf{M}^* &= \sum_{k=1}^n \int_{h_i}^{h_{i+1}} \Lambda \sigma^S \zeta^3 d\zeta, \\
\mathbf{N}_n &= \sum_{k=1}^n \int_{h_i}^{h_{i+1}} \sigma_z \kappa(\zeta) \zeta d\zeta, & \mathbf{Q} &= \sum_{k=1}^n \int_{h_i}^{h_{i+1}} \Lambda \tau_S d\zeta, \\
\mathbf{Q}^* &= \sum_{k=1}^n \int_{h_i}^{h_{i+1}} \Lambda \tau_S \zeta^2 d\zeta & \text{and } \mathbf{Q}^{**} &= \sum_{k=1}^n \int_{h_i}^{h_{i+1}} \Lambda \tau_S \zeta^3 d\zeta,
\end{aligned} \tag{5}$$

where

$$\begin{aligned}
\kappa(\zeta) &= 1 - \zeta \left(\frac{1}{R_\xi} + \frac{1}{R_\eta} \right) + \zeta^2 \left(\frac{1}{R_\xi R_\eta} \right), \\
\Lambda &= \mathbf{I} + \zeta \mathbf{C}_b, & \mathbf{C}_b &= \mathbf{C}_0^{-1} \bar{\mathbf{B}} \mathbf{C}_0, \\
\mathbf{C}_0 &= \begin{bmatrix} \mathbf{a}^1 \mathbf{t}_1 & \mathbf{a}^1 \mathbf{t}_2 \\ \mathbf{a}^2 \mathbf{t}_1 & \mathbf{a}^2 \mathbf{t}_2 \end{bmatrix}, & \bar{\mathbf{B}} &= \begin{bmatrix} \mathbf{a}^2 \mathbf{n}_\eta & -\mathbf{a}^1 \mathbf{n}_\eta \\ -\mathbf{a}^2 \mathbf{n}_\xi & \mathbf{a}^1 \mathbf{n}_\xi \end{bmatrix} & \text{and } \sigma^S &= \begin{bmatrix} \sigma_{xx} & \sigma_{xy} \\ \sigma_{yx} & \sigma_{yy} \end{bmatrix}.
\end{aligned}$$

Here, R_ξ and R_η are the radius of curvature of the shell. The limits h_i and h_{i+1} represent respectively the lower and upper coordinates ζ of the i -th laminate. Here, $(\mathbf{a}^1, \mathbf{a}^2)$ is the dual base associated with the natural base $(\mathbf{a}_1, \mathbf{a}_1)$ tangent to the surface, \mathbf{n} is the normal vector to the surface and $(\mathbf{t}_1, \mathbf{t}_2)$ is the tangent orthogonal base (Batoz and Dhatt, 1992). Moreover, The generalized "stresses" may be expressed as:

$$\begin{aligned}
\mathbf{N} &= \begin{bmatrix} N_{xx} & N_{xy} \\ N_{yx} & N_{yy} \end{bmatrix}, & \mathbf{N}^* &= \begin{bmatrix} N_{xx}^* & N_{xy}^* \\ N_{yx}^* & N_{yy}^* \end{bmatrix}, & \mathbf{M} &= \begin{bmatrix} M_{xx} & M_{xy} \\ M_{yx} & M_{yy} \end{bmatrix}, & \mathbf{M}^* &= \begin{bmatrix} M_{xx}^* & M_{xy}^* \\ M_{yx}^* & M_{yy}^* \end{bmatrix}, \\
\mathbf{Q} &= \begin{Bmatrix} Q_{xz} \\ Q_{yz} \end{Bmatrix}, & \mathbf{Q}^* &= \begin{Bmatrix} Q_{xz}^* \\ Q_{yz}^* \end{Bmatrix} & \text{and } \mathbf{Q}^{**} &= \begin{Bmatrix} Q_{xz}^{**} \\ Q_{yz}^{**} \end{Bmatrix}.
\end{aligned} \tag{6}$$

3. COMPOSITE MATERIAL

Most of the composite shell structures are manufactured with composite materials obtained by the superposition of several laminates. Each laminate is formed by unidirectional fibers in an epoxy matrix whose fibers may be oriented arbitrarily. These composite materials may be modeled as an homogenized orthotropic material, with respect to the fiber oriented system 123, whose constitutive equation may be derived by the application of the rule of mixtures. Thus, each laminate, as illustrated in Fig. 1, is modeled as an anisotropic material relative to a global frame.

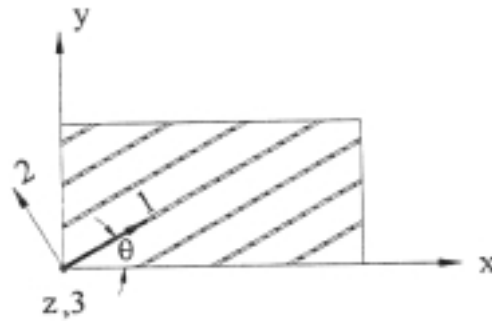


Figure 1 - Unidirectional fiber laminate type

The homogenized orthotropic constitutive equation of the lamina, in the fiber oriented frame is given as:

$$\varepsilon^1 = \begin{Bmatrix} \varepsilon_1 \\ \varepsilon_2 \\ \varepsilon_3 \\ \gamma_{12} \\ \gamma_{13} \\ \gamma_{23} \end{Bmatrix} = \begin{bmatrix} 1/E_1 & -\nu_{12}/E_1 & -\nu_{13}/E_1 & 0 & 0 & 0 \\ & 1/E_2 & -\nu_{23}/E_{21} & 0 & 0 & 0 \\ & & 1/E_3 & 0 & 0 & 0 \\ & & & 1/G_1 & 0 & 0 \\ & sym. & & & 1/G_2 & 0 \\ & & & & & 1/G_3 \end{bmatrix} \begin{Bmatrix} \sigma_1 \\ \sigma_2 \\ \sigma_3 \\ \tau_{12} \\ \tau_{13} \\ \tau_{23} \end{Bmatrix} = S\sigma^1. \quad (7)$$

Since the lamina may be oriented arbitrarily, the local homogenized constitutive equation obtained with respect to the coordinate system 123 must be rotated to a global cartesian system xyz. The rotation transformation is done by the matrix T, whose inverse is given as:

$$T^{-1} = \begin{bmatrix} c^2 & s^2 & 0 & -2cs & 0 & 0 \\ s^2 & c^2 & 0 & 2cs & 0 & 0 \\ 0 & 0 & 1 & 0 & 0 & 0 \\ cs & -cs & 0 & c^2 - s^2 & 0 & 0 \\ 0 & 0 & 0 & 0 & c & -s \\ 0 & 0 & 0 & 0 & s & c \end{bmatrix}, \quad \begin{matrix} c = \cos \theta \\ s = \sin \theta \end{matrix}. \quad (8)$$

Therefore, the constitutive relation of the laminated, in the global coordinate system xyz, is

$$\sigma^x = T^{-1} S^{-1} T^{-T} \varepsilon^x \quad (9)$$

where the stress and strain vectors are defined as $\sigma^x = \{\sigma_x \ \sigma_y \ \sigma_z \ \tau_{xy} \ \tau_{xz} \ \tau_{yz}\}$ and $\varepsilon^x = \{\varepsilon_x \ \varepsilon_y \ \varepsilon_z \ \gamma_{xy} \ \gamma_{xz} \ \gamma_{yz}\}$ (VINSON, J.R. & SIERAKOWSKI, R.L., 1987).

3. OPTIMIZATION PROBLEM

The objective of the problem is to minimize the weight of arbitrary shell structures subjected to a set of stress and side constraints. The design variables are considered to be the thickness of the laminates, t , and the fiber orientation, θ , which form the composite material of the shell. The optimization procedure is performed in a two level procedure:

(a) First level of optimization. The objective is to minimize the fiber orientation angles by minimizing the mean Tsai-Hill effective stress. This problem may be formulated by:

$$\begin{aligned} \min \Phi(\theta) \quad \text{st} \\ -90^\circ \leq \theta \leq 90^\circ \end{aligned} \quad (10)$$

where

$$\Phi(\theta) = \sum_{k=1}^{Nm} \frac{1}{N_{ek}} \sum_{i=1}^{N_{ek}} \sum_{j=1}^{N_{ik}} \sigma_{TH}^l(k, j, i) + \sigma_{TH}^u(k, j, i).$$

The Tsai-Hill failure criteria for a triaxial state, with respect to the axis (1,2,3) may be written as:

$$\begin{aligned} \sigma_{TH} = & \frac{\sigma_1^2}{X_r^2} - \sigma_2\sigma_3 \left(-\frac{1}{X_r^2} + \frac{1}{Y_r^2} + \frac{1}{Z_r^2} \right) + \frac{\sigma_{23}^2}{V_r^2} + \frac{\sigma_2^2}{Y_r^2} - \sigma_1\sigma_3 \left(\frac{1}{X_r^2} - \frac{1}{Y_r^2} + \frac{1}{Z_r^2} \right) + \frac{\sigma_{13}^2}{U_r^2} + \\ & \frac{\sigma_3^2}{Z_r^2} - \sigma_1\sigma_2 \left(\frac{1}{X_r^2} + \frac{1}{Y_r^2} - \frac{1}{Z_r^2} \right) + \frac{\sigma_{12}^2}{S_r^2}. \end{aligned} \quad (11)$$

Here, N_{tm} is the number of material groups (thickness), N_{ek} is the number of elements belonging to the material group k and N_{lk} is the number of lamina belonging to the material group k . Moreover, $\sigma_{TH}^l(k, j, i)$ and $\sigma_{TH}^u(k, j, i)$ are the Tsai-Hill (VINSON, J.R. & SIERAKOWSKI, R.L., 1987) at the bottom and upper face of the i -th element of the j -th lamina of the material group k . The solution of this problem was done by: evaluating the function at every 15 degrees, identifying the set of two intervals, bracketing, that contains the absolute minimum and by using a quadratic interpolation method to determine the optimum angle.

(b) Second level of optimization. The objective is to minimize the thickness of the lamina. In order to solve this class of problems we make use of the Augmented Lagrangian method (BERTSEKAS, D.P., 1982), which can be described by the following procedure:

$$\begin{aligned} \min f(\mathbf{t}) \text{ such that} \\ g_i^{t,\sigma}(\mathbf{t}) \leq 0, \quad i = 1, \dots, m. \end{aligned} \quad (12)$$

Here $f(\mathbf{t})$ is the total mass of the structure and $g_i^{t,\sigma}(\mathbf{t})$, $i = 1, \dots, m$ represents the set of side and Tsai-Hill equivalent stress constraints. The Augmented Lagrangian method is described as:

- Given the initial pair $(\varepsilon^k, \lambda^k)$ for $k=0$, determine the solution to the unconstrained problem: Find \mathbf{t} such that it minimizes the following function:

$$\chi(\mathbf{t}, \lambda^k, \varepsilon^k) = f(\mathbf{t}) + \frac{1}{\varepsilon^k} \sum_{i=1}^m \psi_i(\mathbf{t}, \varepsilon^k, \lambda_i^k)$$

where,

$$\psi_i(\mathbf{t}, \lambda^k, \varepsilon^k) = \begin{cases} g_i(\mathbf{t})(g_i(\mathbf{t}) + \varepsilon^k \lambda_i^k), & \text{if } g_i(\mathbf{t}) \geq -\varepsilon^k \lambda_i^k / 2 \\ -(\varepsilon^k \lambda_i^k / 2)^2, & \text{if } g_i(\mathbf{t}) < -\varepsilon^k \lambda_i^k / 2 \end{cases}, \quad (13)$$

- update the Lagrange multiplier

$$\lambda_i^{k+1} = \max(0, \lambda_i^k - \frac{2g_i(\mathbf{t}^k)}{\varepsilon^k}), \quad (14)$$

- update of the penalty parameter

$$\varepsilon^{k+1} = \max\{\rho\varepsilon^k, \varepsilon_{\min}\}, \text{ for some } 0 < \rho < 1. \quad (15)$$

(c) Verification of convergence. If convergence is not achieved then we return to **(a)** and iterate again.

The objective function is given as:

$$f(t) = \sum_{k=1}^{N_m} \sum_{j=1}^{N_{ek}} \sum_{i=1}^{N_{lk}} \rho_{(k,j)} V_{\zeta}(t)_{(k,j,i)}, \quad (16)$$

where $\rho_{(k,j)}$ is the specific mass of the j -th lamina of the material group k and $V_{\zeta}(t)_{(k,j,i)}$ is the volume of the i -th element determined in the j -th lamina of the material group k . The thickness constraints are given as:

$$g_{(k,j,1)}^t = \frac{1}{t_{(k,j)}^{\inf}} (t_{(k,j)} - t_{(k,j)}^{\sup}) \leq 0 \quad \text{and} \quad g_{(k,j,2)}^t = \left(1 - \frac{t_{(k,j)}}{t_{(k,j)}^{\inf}} \right) \leq 0. \quad (17)$$

The Tsai-Hill effective stress constraints are given by:

$$\frac{\sigma_{(k,j,i)}^l}{\sigma_{(k,j)}^{\sup}} - 1 \leq 0, \quad \frac{1}{\sigma_{(k,j)}^{\sup}} (\sigma_{(k,j)}^{\inf} - \sigma_{(k,j,i)}^l) \leq 0, \quad \frac{\sigma_{(k,j,i)}^u}{\sigma_{(k,j)}^{\sup}} - 1 \leq 0$$

and

$$\frac{1}{\sigma_{(k,j)}^{\sup}} (\sigma_{(k,j)}^{\inf} - \sigma_{(k,j,i)}^u) \leq 0. \quad (18)$$

In order to perform the optimization process, we need to determine the gradient of the objective function and of the inequality constraints. Here, we make use of the direct method for the sensitivity analysis of the structure. By denoting \mathbf{x} to be the vector of the design variables we may represent the discretized equilibrium equation by:

$$[K(\mathbf{x})]\mathbf{u}(\mathbf{x}) = \mathbf{F}, \quad (19)$$

where $[K(\mathbf{x})]$ denotes the stiffness matrix of the structure, $\mathbf{u}(\mathbf{x})$ the nodal displacements and \mathbf{F} the nodal forces. The objective function may be represented in general as:

$$\psi(\mathbf{x}) = \psi(\mathbf{x}, \mathbf{u}(\mathbf{x})). \quad (20)$$

By differentiating this equation we derive,

$$d\psi(\mathbf{x}) = \nabla \psi(\mathbf{x}) d\mathbf{x} = \frac{\partial \psi}{\partial \mathbf{x}} d\mathbf{x} + \frac{\partial \psi}{\partial \mathbf{u}} \cdot \frac{\partial \mathbf{u}}{\partial \mathbf{x}}. \quad (21)$$

Now, by considering the nodal load to be independent of the design variables, we may compute the sensitivity by

$$[K(\mathbf{x})] \frac{\partial \mathbf{u}}{\partial x_i} = - \left[\frac{\partial K(\mathbf{x})}{\partial x_i} \right] \mathbf{u}(\mathbf{x}), \quad i = 1, n \quad \text{for} \quad \mathbf{u} \in R^n. \quad (22)$$

The inequality constraints may be expressed in general as:

$$g_i(\mathbf{x}) = G_i(\mathbf{x}, \mathbf{u}(\mathbf{x})), \quad i = 1, N_g. \quad (23)$$

Here, again we compute the gradient by

$$\nabla g_i(\mathbf{x}) = \frac{\partial G_i}{\partial x_k} + \frac{\partial G_i}{\partial u_j} \cdot \frac{\partial u_j}{\partial x_k}, \quad i = 1, N_g, k = 1, N_x \text{ and } j = 1, n. \quad (24)$$

3. NUMERICAL RESULTS

In the discretization of the problem we employ the Galerkin Finite Element method and use a Quad9 isoparametric element with a selective reduced integration approach. With the objective of showing the performance of the method we solve two problems, which are:

(a) **Laminate cylinder.** Here, we consider the problem proposed by (Haas and Lee, 1987), also analyzed by (Wilt et al, 1990) and illustrated in Fig. 2. It consists of a composite cylinder under pressure with clamped edges. The internal pressure $q_0 = 6.41\pi$, with dimensions: $L=2R=20$. The material properties are given by: $E_1=7.5E+06N/m^2$, $E_2 = E_3=2.0E+06N/m^2$, $G_{12}=1.25e+06N/m^2$, $G_{13}=G_{23}=6.25e+05N/m^2$, $\nu_{12}=\nu_{13}=\nu_{23}=0.25$.

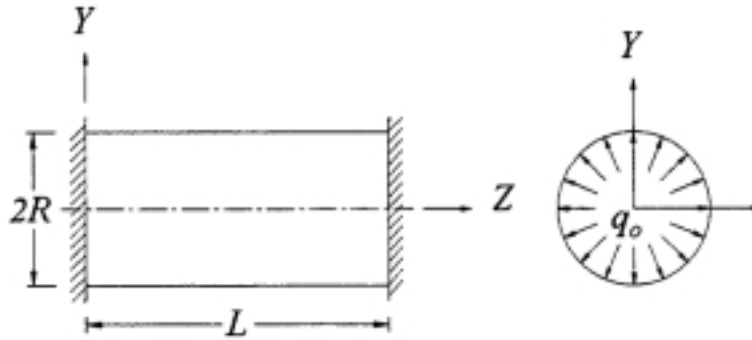


Figure 2 - Clamped cylinder under internal pressure

The cylinder is analyzed for three different laminates: $[0]$, $[45/-45]_s$ and $[0/90]_s$. The result is presented in Tabs. 1 obtained for meshes with 6×6 and 10×10 elements. they are also compared with the results obtained by (Hass and Lee, 1987) and (Wilt et all, 1990).

Table 1. Maximum radial displacement

angle	Disp. wx100 6x6	Disp. wx100 10x10	Disp. wx100 Wilt	Disp. wx100 Hass
$[0]$	0.3750	0.3745	0.3758	0.3781
$[45/-45]_s$	0.1777	0.2095	0.2331	0.2402
$[0/90]_s$	0.2064	0.1623	0.1787	0.1783

The radial displacement along the generator of the cylinder for the tree cases of laminates is shown in Fig. 3. For a rate $h/L=20/100$.

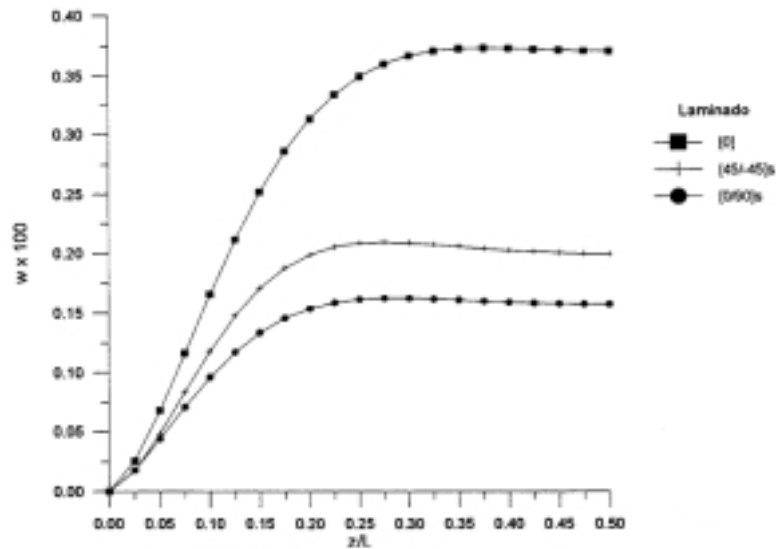


Figure 3 - Radial displacement along the cylinder generator

(b) **Pressure Vessel with a semi spherical head.** In this problem we consider the pressure vessel illustrated in Fig. 4. Here, we use a regular mesh of 135 elements, 9 along the circumference and 15 in the Z direction. From those 15, 6 elements are in the cylindrical part and 9 in the cover head. The material is considered to be isotropic with the following properties: $E=210\text{Gpa}$, $G=84\text{Gpa}$, $\nu=0.25$. The Tsai-Hill criteria is defined by: $X_T = 250\text{MPa}$, $S_r = 165\text{MPa}$, $X_T = X_C = Y_T = Y_C = Z_T = Z_C$ and $S_r = U_r = V_r$. The cylinder has a radius $R=0.11\text{m}$, a length $L=0.40\text{m}$. The semi spherical heads have a radius $R=0.09\text{m}$ and have a rigid valve at the end. The internal pressure is $q_0=20\text{Mpa}$.

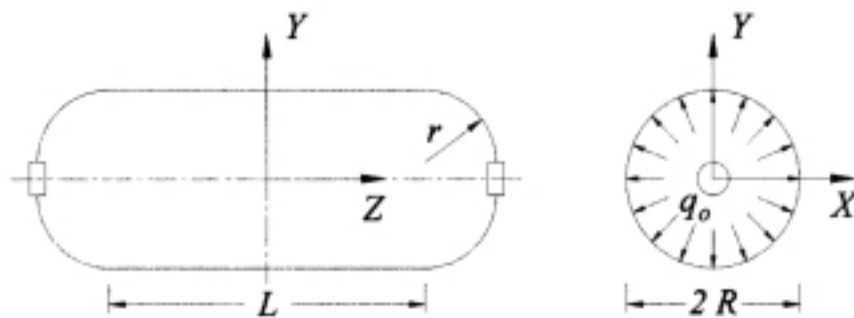


Figure 4 - Pressure Vessel with semi spherical head

The structure is divided into 4 material groups, where the first group represents the cylindrical part of the structure with 54 elements, and the other 3 groups are used in semi spherical head. The head cover is segmented into 9 rings with 9 elements for each ring in the circumferential direction. Those rings are numbered starting from the junction with the cylinder. The second material group, containing 18 elements, is formed by the rings 1 and 2. The third group, containing 45 elements, is formed by the rings 3,4,5,6 and 7. The fourth group, containing 18 elements, is formed by the rings 8 and 9. The disposition of the material groups is shown in Fig. 5.

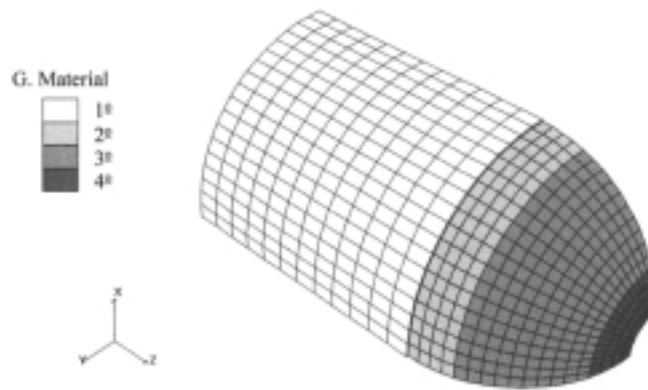


Figure 5 - Material group disposition

The initial and final material group thickness is given in table 2. The optimization process has allowed a mass reduction of 15.4% of the initial mass. The density of the material is $\rho=7500\text{Kg/m}^3$.

Material group	1°	2°	3°	4°
Initial thickness [mm]	9.00	6.5	6.5	6.5
Final thickness [mm]	8.05	4.56	4.47	5.66

The distribution of the Tsai-Hill, in the pressure vessel, considering the initial thickness is shown in Fig. 6.

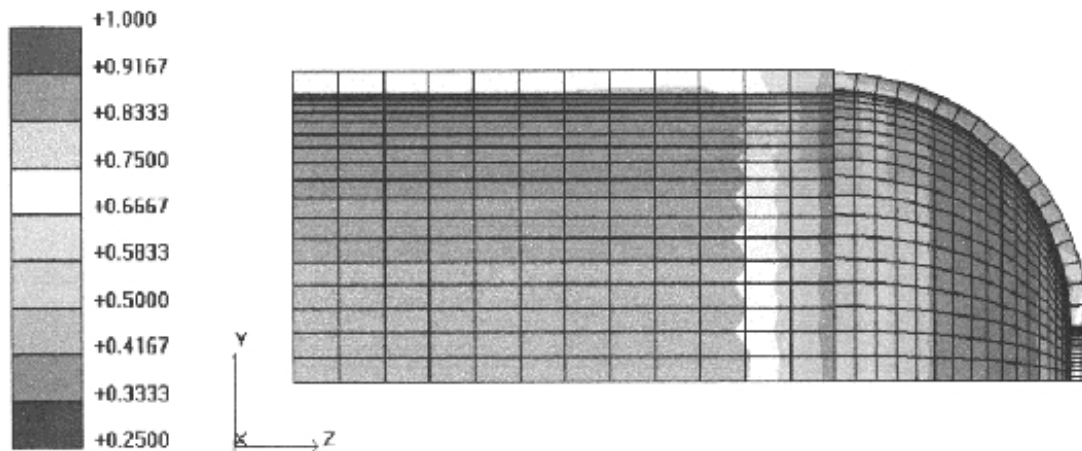


Figure 6 - Tsai-Hill stress distribution

4. CONCLUSION

Now, due to the growing use of laminate composite materials and the necessity to reduce the cost of the material it becomes even more relevant to design optimized shell structures. Moreover, considering that one of the main failure mode is related to the inter laminate shear stresses, the consideration of a higher order theory is of primary importance. An improved shear stress distribution can be obtained by a post-processing method which also correct the boundary condition at the free surfaces. Now, since real shell structures in general employ a large number of degrees of freedom in their discretization and since the optimization process requires a large number of iterations, it is of fundamental importance to improve the algorithm by reducing the time of the optimal design.

5. REFERENCES

- BATOZ, J. & DHATT, G., 1992, *Modélisation des Structures par Éléments Finis*, Hermes.
- BERTSEKAS, D.P., 1982, *Constrained Optimization and Lagrange Multiplier Methods*, Academic Press, San Diego.
- FEIJÓO, R.A. & TAROCO, E., 1993, *Introducción al Análisis de Sensibilidad*, Notas de Curso, Laboratório Nacional de Computação Científica, Rio de Janeiro.
- HAAS, D.J. & LEE, S.W., 1987, A Nine-node Assumed Strain Finite Element for Composite Plates and Shells, *Computers & Structures*, Vol. 26, No.3, pp.445-452.
- KANT, T., 1982, Numerical Analysis of Thick Plates, *Computer Methods Applied Mech. Engng.* vol. 31, pp 1-18.
- PANDYA, B.N. & KANT, T., 1988, A Refined Higher-Order Generally Orthotropic C° Plate Bending Element, *Computers & Structures*, Vol.28, No.2, pp.119-133.
- REDDY, J. N., 1984, Simple Higher-Order Theory for Laminated Composite Plates, *Journal of Applied Mechanics*, vol. 51, pp. 745-752.
- SIVAKUMARAN, K.S., CHOWDHURY, S.H. & VAJARASATHIRA, K., 1994, Some Studies on Finite Elements for Laminated Composite Plates, *Computers & Structures* vol. 52, No. 4, pp 729-741.
- VINSON, J.R. & SIERAKOWSKI, R.L., 1987, *The Behavior of Structures Composed of Composite Materials*, Martinus Nijhoff Publishers, Dordrecht.
- WILT, T.E., SALEEB, A.F. & CHANG, T.Y., 1990, a Mixed Element for Laminated Plates and Shells, *Computers & Structures*, Vol.37, No.4, pp.597-611.